Cell Cycle Control of Microtubule-based Membrane Transport and Tubule Formation In Vitro

Viki J. Allan and Ronald D. Vale

Department of Pharmacology, University of California, San Francisco, California 94143

Abstract. When higher eukaryotic cells enter mitosis, membrane organization changes dramatically and traffic between membrane compartments is inhibited. Since membrane transport along microtubules is involved in secretion, endocytosis, and the positioning of organelles during interphase, we have explored whether the mitotic reorganization of membrane could involve a change in microtubule-based membrane transport. This question was examined by reconstituting organelle transport along microtubules in *Xenopus* egg extracts, which can be converted between interphase and metaphase states in vitro in the absence of protein synthesis. Interphase extracts support the microtubule-dependent formation of abundant polygonal networks of membrane tubules and the transport of small vesicles. In metaphase extracts, however, the plus end– and minus end–directed movements of vesicles along microtubules as well as the formation of tubular membrane networks are all reduced substantially. By fractionating the extracts into soluble and membrane components, we have shown that the cell cycle state of the supernatant determines the extent of microtubule-based membrane movement. Interphase but not metaphase *Xenopus* soluble factors also stimulate movement of membranes from a rat liver Golgi fraction. In contrast to above findings with organelle transport, the minus end–directed movements of microtubules on glass surfaces and of latex beads along microtubules are similar in interphase and metaphase extracts, suggesting that cytoplasmic dynein, the predominant soluble motor in frog extracts, retains its force-generating activity throughout the cell cycle. A change in the association of motors with membranes may therefore explain the differing levels of organelle transport activity in interphase and mitotic extracts. We propose that the regulation of organelle transport may contribute significantly to the changes in membrane structure and function observed during mitosis in living cells.

MANY membranous organelles during interphase have defined structures and positions within the cytoplasm. The Golgi apparatus is clustered around the microtubule organizing center in the perinuclear area, and consists of stacked membrane cisternae and associated tubules (Rambourg and Clermont, 1990). The ER on the other hand, is organized as a system of interconnecting tubules and cisternae (Terasaki et al., 1986) that stretches from the nucleus to the cell periphery. Lysosomes can also display tubular shapes (Swanson et al., 1987), and the endosomal compartment has recently been described as an interconnected system of tubules (Hopkins et al., 1990). The location of lysosomes and late endosomes in fibroblasts is generally perinuclear (Matteoni and Kreis, 1987; Herman and Albertini, 1984), although peripheral localization has been described under certain conditions (Heuser, 1989).

The establishment and maintenance of organelle position in higher eukaryotes are active processes that require microtubules. The Golgi apparatus reaches the perinuclear area by moving along microtubules towards their minus ends located at the centrosome (Ho et al., 1989), while the ER extends towards the plus ends of microtubules, which are generally located in the cell periphery (Lee et al., 1989; Lee and Chen, 1988). Two microtubule-based motor proteins kinesin, which promotes plus end–directed movement (Vale et al., 1985*a*), and cytoplasmic dynein, which powers minus end–directed movement (Paschal et al., 1987), are thought to be good candidates for organelle transport motors (Schnapp and Reese, 1989; Schroer et al., 1988, 1989; Pfister et al., 1989). These (or related) motor proteins may also generate the tubular configurations of the Golgi apparatus (Cooper et al., 1990), the ER (Lee et al., 1989), the intermediate (salvage) compartment (Lippincott-Schwartz et al., 1990), and lysosomes (Swanson et al., 1987). Consistent with this proposal, tubular lysosomes collapse when an antikinesin mAb is injected into the cytoplasm (Hollenbeck and Swanson, 1990). Microtubule transport is also used to bring endosomes and lysosomes to the center of the cell for fusion (Bomsel et al., 1990; Gruenberg et al., 1989) and to deliver Golgi-derived vesicles to the cell periphery (Arnheiter et al., 1984; Cooper et al., 1990). Taken together, these observations reveal the importance of microtubule-based organelle transport for organizing membrane compartments within the interphase cytoplasm.

Viki J. Allan's present address is Laboratory of Molecular Biology, Medical Research Council, Cambridge CB2 2QH, England.

During the transition from interphase to mitosis in higher eukaryotes, membrane organization changes dramatically. Concomitant with nuclear membrane breakdown, the Golgi apparatus fragments (Robbins and Gonatas, 1964; Colman et al., 1985), and the Golgi remnants no longer interact with microtubules and become randomly distributed in the cytoplasm (Lucocq et al., 1989). This fragmentation process may be necessary in order for single copy organelles, such as the Golgi, to be partitioned equally between both daughter cells (Warren, 1985). The extent to which the ER fragments during mitosis is somewhat variable in different cell types (Robbins and Gonatas, 1964; Zeligs and Wollman, 1979). Like the Golgi apparatus, however, most ER components seem to be excluded from the spindle and aster regions in vertebrate cells (Robbins and Gonatas, 1964; Roos, 1973), as are other organelles such as mitochondria, secretory granules, endosomes, and lysosomes (Matteoni and Kreis, 1987; Rebhun, 1972; Robbins and Gonatas, 1964; Tooze and Burke, 1987). As these structural changes are taking place, many functional properties of intracellular membrane compartments are inhibited, including protein secretion (Ceriotti and Colman, 1989; Featherstone et al., 1985; Warren et al., 1983), pinocytosis (Berlin and Oliver, 1978), and receptor-mediated endocytosis (Pypaert et al., 1987; Warren et al., 1984). During telophase, these morphological and functional changes are reversed, and the interphase pattern of organelle–microtubule interactions begins to be reestablished.

The molecular basis of the changes in organelle structure and function during mitosis is unknown. One hypothesis is that membrane fusion is inhibited but membrane budding continues during mitosis, thereby leading to organelle fragmentation and inhibition of membrane traffic (Warren, 1985). The reduction in endosomal fusion in metaphase versus interphase *Xenopus* extracts (Tuomikoski et al., 1989) is consistent with this hypothesis.

An inhibition of microtubule-based organelle transport during mitosis also could conceivably lead to a dispersion of organelles and an inhibition of membrane traffic. One way to test whether organelle transport is reduced during mitosis is to reconstitute organelle transport in extracts in which the cell cycle status can be controlled. An ideal system for such studies is the *Xenopus laevis* egg, extracts of which will undergo single (Lohka and Maller, 1985) or multiple (Murray and Kirschner, 1989) cell cycles in vitro. These extracts have proved useful for dissecting complex processes such as nuclear envelope breakdown (e.g., Newport, 1987; Newport and Spann, 1987), mitotic inhibition of endosomal fusion (Tuomikoski et al., 1989), and microtubule dynamics (Belmont et al., 1990; Verde et al., 1990), as well as for analyzing the regulatory mechanisms of the cell cycle itself (Murray and Kirschner, 1989; Nurse, 1990). In this study, we find extensive tubular membrane network formation and vesicle movement in interphase, but not in mitotic extracts from *Xenopus* eggs. Thus, organelle transport along microtubules is regulated by a posttranslational switch that is controlled by the cell cycle.

Materials and Methods

Materials

Taxol was a gift from Dr. M. Suffness at the National Cancer Institute. Monoclonal antibeta tubulin (YL1/2) was obtained from Amersham Corp. (Arlington, IL), and rhodamine-labeled goat anti-mouse IgG was obtained from Accurate Sci. Co. (Westburg, NY). 3,3'-dihexyloxacarbocyanine iodide ($DiOC_6[3]$)[1] was purchased from Molecular Probes, Inc. (Eugene, OR). AMP-PNP and ^{32}P-gamma ATP were obtained from Boehringer Mannheim Biochemicals (Indianapolis, IN) and ICN K & K Laboratories Inc. (Costa Mesa, CA), respectively. Ultra-pure sucrose and Hepes (biochemika grade) were obtained from BRL (Gaithersburg, MD) and Fluka (Ronkonkoma, NY), respectively. All other reagents were purchased from Sigma Chemical Co. (St. Louis, MO).

Preparation of Xenopus Egg Extracts

Extracts arrested in metaphase of meiosis II by CSF were prepared as described (Murray and Kirschner, 1989). Interphase extracts were also prepared as described (Murray and Kirschner, 1989), except that cycloheximide (100 μg/ml) was added during the final egg washes and the breakage step to ensure complete interphase arrest. Both extracts (~75–90 mg/ml protein concentration) were stored in liquid nitrogen.

Meiotic extracts prepared from metaphase-arrested eggs were induced to enter interphase by adding 1:50 vol of 20 mM $CaCl_2$, 100 mM KCl, 1 mM $MgCl_2$ and cycloheximide to 100 μg/ml (to inhibit cyclin synthesis), and incubating at 23°C for 30 min. After addition of EGTA to 0.4 mM, the sample was transferred to ice. Interphase extracts from activated eggs were induced to enter mitosis by incubating for 45 min at 23°C with 1 mM of cyclinΔ90, a nondegradable sea urchin cyclin B lacking the NH_2-terminal 90 amino acids (Murray et al., 1989). CyclinΔ90 was kindly supplied as purified bacterially expressed protein by Michael Glotzer (Department of Biochemistry, University of California at San Francisco).

Interphase and metaphase extracts were fractionated by centrifugation to yield crude organelles and high-speed supernatants as follows. The extracts were diluted on ice with 2 vol of acetate buffer (100 mM K-acetate, 3 mM Mg-acetate, 5 mM EGTA, 10 mM HEPES, pH 7.4, 150 mM sucrose) containing an energy mix for replenishing nucleotide triphosphates (1 mM MgATP and 7.5 mM creatine phosphate). To prepare supernatants, the diluted extracts were centrifuged in an airfuge (Beckman Instruments, Palo Alto, CA) at 28 p.s.i. for 30 min at 4°C (final protein concentration 18–25 mg/ml). To prepare organelles, the diluted extract was layered over 50 μl acetate buffer containing 300 mM sucrose plus energy mix and centrifuged as above. The organelle layer on top of the glycogen granule and ribosome pellet was resuspended in acetate buffer plus energy mix to 40% of the original extract volume.

The cell cycle state of extracts and supernatants was monitored routinely by assaying histone kinase activity and occasionally by examining the state of chromatin condensation in demembranated *Xenopus* sperm nuclei (Murray and Kirschner, 1989). Histone kinase activities are expressed throughout as pmol ATP incorporated per μl of undiluted extract per minute. Standardization by original extract volume rather than by protein concentration allows direct comparison of histone kinase activities in extracts with those in high speed supernatants.

Preparation of a Stacked Golgi Fraction from Rat Liver

A stacked Golgi fraction was prepared from male or female rat liver using the method described by Leelavathi et al. (1970) with the following modifications. Livers were homogenized in 1 ml of 0.25 M sucrose in acetate buffer with 10 μg/ml protease inhibitors per gram wet weight. Acetate buffer plus 1 μg/ml protease inhibitors was used to make all other sucrose solutions. The smooth membrane fraction from the first gradient was made to 1.25 M sucrose and was then layered onto a 1.4 M sucrose cushion and overlaid with 1.1 and 0.25 M sucrose. The stacked Golgi membrane fraction (~5 mg/ml) was collected from the 1.1 M/0.25 M sucrose interface and stored in liquid nitrogen.

Motility Assays

Motility was assayed in 6–8-μl perfusion chambers as described (Vale and Toyoshima, 1988), except that Scotch tape was used as a spacer between the slide and the coverslip. Motility assays were generally performed using 3 μl of crude extract diluted with 6 μl of acetate buffer, or with 8 μl of high-speed supernatant combined with 0.5–1 μl of crude *Xenopus* organelles or

1. *Abbreviations used in this paper*: CSF, cytostatic factor; DIC, differential interference contrast; $DiOC_6(3)$,3,3'-dihexyloxacarbocyanine iodide.

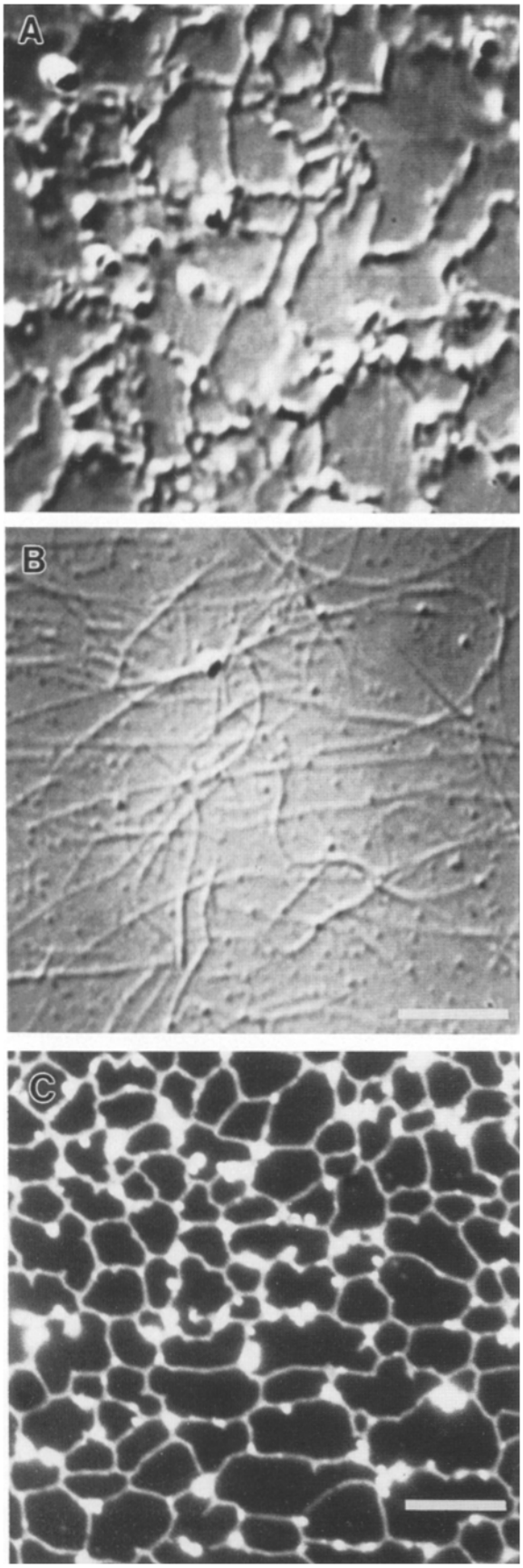

Figure 1. Tubular membrane network formation in interphase extracts. Interphase extracts incubated with microtubules in a microscope perfusion chamber for 20 min formed extensive tubular networks which are visualized in *A* by DIC microscopy. These tubules are membranous, as they are solubilized by flowing through acetate buffer containing 0.1% Triton X-100 and 20 μM taxol, revealing microtubules bound to the glass coverslip (*B*). (Different, but typical fields are shown in *A* and *B*). Tubular networks incorporated the lipophilic dye, $DiOC_6(3)$(5 μg/ml in acetate buffer), as shown by fluorescence microscopy (*C*). These interphase extracts, prepared from activated eggs, were incubated with microtubules as described in Materials and Methods. Bars, 5 μm.

rat liver Golgi fraction. In a few cases, 4 μl of extract was diluted with 4 μl of 80 mM Pipes/KOH, 1 mM $MgCl_2$, 1 mM EGTA, pH 6.8. If a sample already in the perfusion chamber was exchanged, 15 μl of new sample was flowed through to avoid dilution effects.

Unlike interphase extracts, which spontaneously polymerize microtubules, metaphase extracts diluted in acetate buffer did not polymerize microtubules unless a small number of nucleating microtubule were supplied (see also Verde et al., 1990). Nucleating microtubules were therefore supplied to both interphase and metaphase extracts in one of two ways. (*a*) The glass surface of the chamber was first precoated with 20-fold diluted extract, and then a 100–250-μg/ml solution of taxol-stabilized, bovine brain microtubules (prepared as described [Vale and Toyoshima, 1988]) was perfused into the chamber and incubated at 23°C for 2 min so that the microtubules bound to the coated glass surface. Unbound microtubules were washed out and the sample to be tested was flowed into the chamber. (*b*) Bovine microtubules (1.25 μg/ml) were added directly to the extract to act as nucleation centers for the polymerization of endogenous tubulin. Both methods resulted in the formation of similar numbers of microtubules in interphase and metaphase extracts or extract supernatants and yielded equivalent results with respect to the membrane transport observations reported in this study. It should be noted that metaphase extracts contain an activity that severs taxol-stabilized, bovine microtubules (Vale, 1991). The severed fragments, however, act as nucleating sites for polymerization of endogenous microtubules, which are more resistant to severing.

Organelle motility in the perfusion chamber remained active for at least 3 h at room temperature. Parallel incubations were performed in microcentrifuge tubes, and aliquots were taken for histone kinase assays at the times (indicated in the legend) when vesicle movement or tubule formation were assayed. The direction of vesicle movement was assayed using axoneme-nucleated microtubules. Salt-washed, dynein-depleted axonemes, prepared from sea urchin sperm as described (Gibbons and Fronk, 1979), were flowed into a perfusion chamber to which they adhered. When *Xenopus* extracts or supernatants were subsequently added, tubulin polymerized from only one end of the axoneme. This was determined to be the plus end by assaying the direction of movement of carboxylated beads coated with purified squid brain kinesin (Vale et al., 1985*b*).

Soluble motor protein activity was assayed by preincubating carboxylated beads (0.11 μm; Polysciences no. 16688, diluted 1:100 from a 5% solid stock) in metaphase or interphase high-speed supernatant for 5 min at 23°C. The bead mixture was flowed into a perfusion chamber containing microtubules formed during a prior 5-min incubation of axonemes with interphase or mitotic high-speed supernatant. Microtubule movement on glass in the presence of supernatants was performed as previously described (Vale et al., 1985*a*).

Microscopy and Photography

Organelle motility was monitored by differential interference contrast microscopy (DIC) using a Zeiss Axioplan equipped with a 100 W mercury arc lamp, a 1.4 NA condensor and a 63×, 1.4 NA Planapochromat objective. Images were projected onto the target of a Hamamatsu Newvicon camera using a 1.25× or 1.6× optivar and a 4× eyepiece. Contrast was enhanced with an Imaging Technology 151 processor, and images were recorded in real time using either a 3/4″ U-matic Sony VO-5800H or a 1/2″ Panasonic NV-8950 video recorder. Single frame images were stored digitally on an AT-based computer after capturing two-frame averages using the 151 image processor. Digital images were converted to Macintosh format, reduced or enlarged, and then mounted side-by-side using IMAGE 1.28 software, a public domain program. Final images were transferred to Panatomic-X film using IMAGEQ software and a Macintosh montage FR1 film recorder.

Fluorescence microscopy was performed on a Zeiss Axioplan by illuminating the specimens with a 100 W mercury arc lamp and a 40×, 0.9

NA Plan-neofluor multi-immersion objective through an epi-fluorescence path. Images were recorded either directly onto 35 mm film or by using a Hamamatsu silicon-intensified target camera (C-2400) and storing single images as described above.

Data Analysis

All data analysis was performed on DIC images recorded onto video tape in real time. Rates of organelle and bead movement and of microtubule gliding on glass were obtained from video tape using an interactive AT-based computer program (Sheetz et al., 1986). The lengths of membrane tubules were measured first by recording >25 random video fields per sample (unless noted) onto video tape, and then tracing the networks manually from the monitor onto acetate sheets. The total length of tubules is expressed per 25 × 32 μm video field. Vesicle movements were quantitated either by counting movements on individual microtubules or by counting movements within a 10.8 × 13.8 μm video field. In both cases, microtubules were traced onto acetate sheets and their length measured as above. Movement is expressed as the number of movement events per min per linear length (μm) of microtubules in the field of view.

EM

25 μl of the rat liver stacked Golgi fraction was thawed and then fixed with 650 μl of 2% EM grade glutaraldehyde and 1% acrolein in 120 mM cacodylate buffer (pH 7.4) on ice for 12 h. The fixed membranes were then centrifuged in 650 μl SW 50.1 tubes with adaptors at 120,000 g_{av} for 50 min at 4°C. The pellet was processed as described (Huttner et al., 1983). Sections were viewed in a Joel 100c electron microscope.

Results

Preparation of Interphase and Metaphase Extracts

Several types of egg extracts were used in these studies (Murray and Kirschner, 1989). Metaphase extracts were prepared from unfertilized *Xenopus* eggs stably arrested in metaphase of meiosis II by the cytostatic factor (CSF), which is the *Xenopus* form of the c-mos proto-oncogene (Sagata et al., 1989). When such eggs are fertilized or activated by electric shock, calcium influx leads to CSF degradation and progression into interphase. Extracts prepared from such activated eggs display many interphase characteristics (Murray and Kirschner, 1989). This interphase extract can be converted in vitro to a mitotic metaphase state by adding a nondegradable cyclin (cyclinΔ90), the protein responsible for initiating mitosis. Metaphase extracts prepared from CSF-arrested eggs can also be converted to an interphase state in vitro by adding calcium (to inactivate CSF) and cycloheximide (to prevent cyclin synthesis). The ability to manipulate an extract's cell cycle state in vitro enabled us in this study to compare the properties of interphase and metaphase states using an extract prepared from one batch of eggs. The cell cycle status of each extract was determined by measuring the phosphorylation of histone H1 (an activity of $p34^{cdc2}$ kinase in the extract).

For all experiments reported below, we find that metaphase extracts prepared from metaphase-arrested eggs or converted from interphase extracts in vitro behaved identically. Similarly, interphase extracts prepared either from activated eggs or converted in vitro from metaphase extracts produced indistinguishable results. We therefore refer in the text below to extracts as being metaphase or interphase; their exact method of preparation can be found in the figure and table legends. All extracts were prepared in the presence of cycloheximide except those made directly from metaphase-arrested eggs. The latter extracts were therefore routinely incubated with cycloheximide for 30 min before an assay, although identical results were obtained in the absence of the drug.

Tubular Membranes Form in Interphase but Not in Metaphase Extracts

When interphase extracts were incubated with microtubules in a microscope perfusion chamber, an extensive network of tubules formed on top of the microtubule-coated glass coverslip within 30 min (Fig. 1 *A*). These tubular networks were solubilized by 0.1% Triton X-100 (Fig. 1 *B*) and were labeled by the lipophilic dye $DiOC_6(3)$ (Fig. 1 *C*), indicating that they are membranous structures. These tubular membrane networks were composed of polygons of tubules with three-way branch points, a pattern that resembles the structure of the ER in vivo (Lee and Chen, 1988). The formation of similar tubular membrane networks has been observed in chicken embryo fibroblast extracts in the presence of microtubules (Dabora and Sheetz, 1988).

Tubular membrane networks require microtubules for their genesis; either taxol-stabilized, bovine brain microtubules or endogenously polymerized, *Xenopus* microtubules will suffice for this process. Microtubules were supplied either by precoating the perfusion chamber with bovine microtubules and then flowing in extract, or by adding bovine microtubule fragments to the extract to stimulate endogenous polymerization. If no bovine microtubules were added and the extract was incubated with 20 μM colcemid to prevent the polymerization of endogenous tubulin, network formation did not take place.

Membrane tubules and networks were generated by a microtubule-based transport process. Membrane tubules, as observed by DIC microscopy, extended from large amorphous membranes attached to the glass by moving along microtubules (Fig. 2) at an average velocity of 1.45 μm/s (± 0.2 SD). Small membrane vesicles (<0.2 μm) moved at a rate similar to that of membrane tubules (1.34 ± 0.21 μm/s), as was also observed in chick embryo fibroblast extracts (Dabora and Sheetz, 1988). Several treatments that inhibit microtubule motors (Dabora and Sheetz, 1988; Vale et al., 1985*a*), such as ATP depletion, AMP-PNP, and 250 μM vanadate, all inhibited formation of tubular membrane networks (Table I) and vesicle movement in interphase extracts. Low concentrations of vanadate (25 μM) had little effect on network formation or vesicle movement. Treatment with 1 mM NEM reduced network formation while vesicle movement continued; treatment with 5 mM NEM blocked both activities.

In addition to the requirement for microtubules and motors, the formation of polygonal networks also appears to involve membrane fusion. An early step in the process seems to involve the fusion of the small vesicles to form larger membrane reservoirs from which tubules extended. The formation of three-way branch points (Fig. 1, *A* and *C*) as two tubules cross over also appears to be mediated by fusion, as previously reported and discussed (Dabora and Sheetz, 1988; Vale and Hotani, 1988). Two potent inhibitors of membrane fusion in vitro (1 mM NEM; 40 μM GTPγS) (Balch, 1989) impair membrane network formation (Table I), with no substantial effect upon the movement of small vesicles along microtubules.

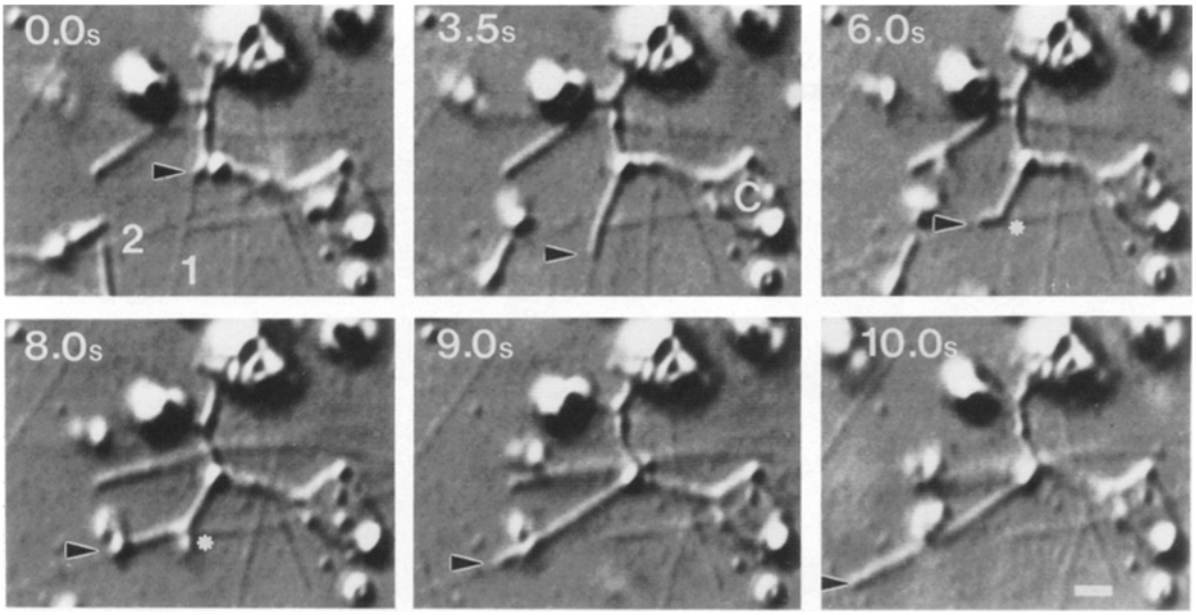

Figure 2. Membrane tubules extend by moving along microtubules. An interphase extract (prepared by adding calcium to a metaphase-arrested extract (Materials and Methods) was diluted with 5 vol of acetate buffer containing energy mix and flowed into a chamber precoated with bovine microtubules. Tubule extension was visualized by DIC microscopy and recorded onto video tape in real time. A tubule (the tip of which is marked with an arrowhead) extends along microtubule 1. (Note: microtubule 1 later dissociates from the glass surface at ~6 s.) Between 3.5 and 6.0 s, this membrane tubule elastically recoils back and then begins to move along microtubule 2. The tubule also has a static attachment point to microtubule 2 (*asterisk*) that releases after 8.0 s. A number of other membrane tubules can be seen in this series, as can a small membrane cisterna (marked *c*). Bar, 1 μm.

Having established that the membrane tubule formation in interphase extracts occurs by a microtubule-based motility process resembling that described by Dabora and Sheetz (1988), we then examined whether a similar phenomenon occurs in metaphase extracts. In contrast to the results with interphase extracts, very little membrane network formation was observed in metaphase extracts, despite the presence of similar numbers of microtubules (Fig. 3). Quantitation of network extent by measuring the total length of membrane tubules per video field revealed a 98% reduction in tubule formation in metaphase when compared to interphase extracts (Table II). When interphase and metaphase extracts were mixed in varying proportions, the amount of tubule formation did not increase linearly with the amount of interphase extract; rather, a 25% contribution of metaphase extract had a substantial inhibitory effect (data not shown). Also, in contrast to the interphase extracts, vesicle movements and membrane tubule extensions along microtubules were very rarely seen in metaphase extracts. It was difficult, however, to see small vesicles clearly due to the presence of large quantities of ribosomes and glycogen granules in the extracts, which degrade the DIC image. Quantitation of vesicle movements was therefore performed using supernatants and isolated membrane fractions, as described in the following section.

Table I. Pharmacology of Membrane Network Formation and Vesicle Movement in Interphase Extracts

Treatment	Membrane tubules		Transport rate
	μm/field	*% control*	*μm/s*
Control	145.1	100.0	1.34 ± 0.21
Apyrase	11.4	7.8	0
AMP-PNP, 3 mM	21.9	15.1	0
NEM, 1 mM	30.6	21.1	1.10 ± 0.28
NEM, 5 mM	9.8	6.7	0
Vanadate, 25 μM	124.8	86.0	1.22 ± 0.20
Vanadate, 250 μM	19.0	13.1	0
GTPγS, 40 μM	22.8	15.7	1.46 ± 0.20
EGTA, 20 mM	115.0	79.3	1.24 ± 0.26

Pharmacology of membrane network formation and vesicle movement in interphase extracts. An extract from metaphase-arrested eggs was converted to an interphase state (see Materials and Methods), diluted 1:1 with 80 mM Pipes, 1 mM $MgCl_2$, and 1 mM EGTA, and flowed into a perfusion chamber precoated with bovine microtubules. Movement of vesicles and the formation of membrane tubule networks were observed by DIC microscopy and recorded onto video tape in real time. The total length of membrane tubules per video field was analyzed after a 5-min incubation at 23°C (6–12 fields per treatment). The rates of vesicle movement are the mean of 25–30 movements measured during a 5–10-min time period (±SD); 0 indicates that no movement was observed during this time interval. Sodium orthovanadate, EGTA, and AMP-PNP were each added to the extract just before flowing it into the chamber. To deplete endogenous ATP, the interphase extract was incubated with 5 U/ml apyrase for 30 min at 23°C. Incubations with NEM were performed for 10 min at 23°C followed by quenching with 15 mM DTT (which itself had no effect on tubule formation or vesicle movement) for 15 min on ice. GTPγS was preincubated with the extract for 40 min on ice.

Interphase but Not Mitotic Supernatants Stimulate Tubule Formation and the Movement of Small Vesicles from Isolated Membranes

To determine whether the lack of membrane-tubule formation in mitotic extracts was due to a property of the membrane, the cytosol, or both, metaphase and interphase extracts were separated by centrifugation into high-speed supernatants and organelle fractions, which were then mixed in different combinations. High-speed supernatants from either metaphase or interphase extracts contained very few small vesicles and

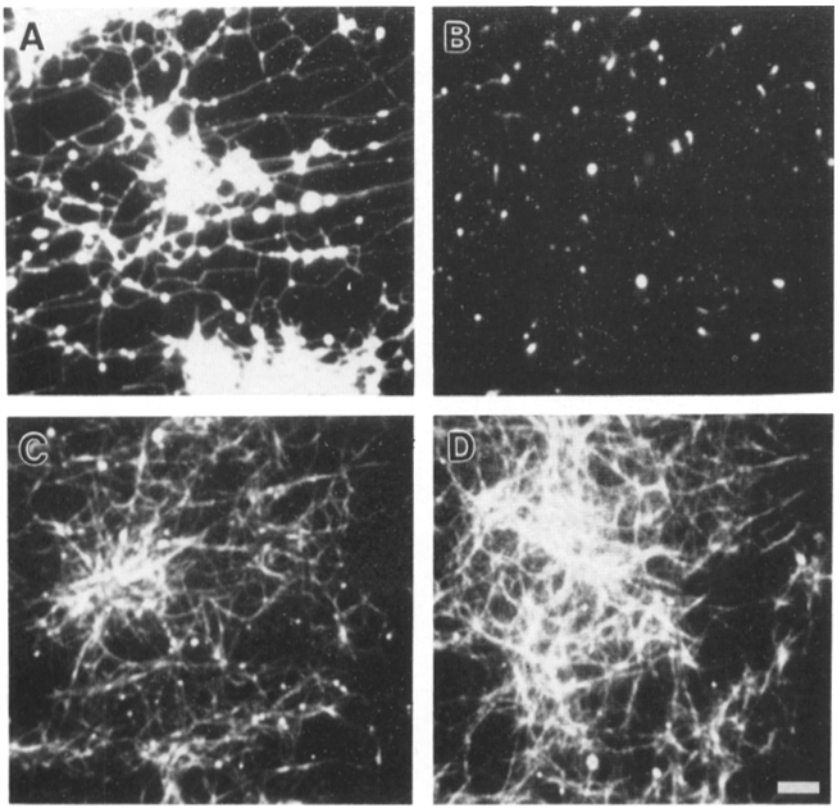

Figure 3. Tubular membrane network formation is inhibited in metaphase extracts. An interphase extract was prepared from activated eggs. One-half of the extract was converted to a metaphase state by incubating with cyclinΔ90, as described in Materials and Methods (*B* and *D*). The other half of the extract went through a mock incubation and remained in an interphase state (*A* and *C*). Both extracts were diluted with 2 vol of acetate buffer and flowed into perfusion chambers precoated with bovine microtubules. After 20 min at 23°C, both samples were labeled with $DiOC_6(3)$ (*A* and *B*) by first washing out excess extract with acetate buffer plus 20 μM taxol and then flowing through 5 μg/ml $DiOC_6(3)$ in acetate buffer. After recording images, the microtubules in the same perfusion chambers were fixed with 1% paraformaldehyde, 0.01% glutaraldehyde in acetate buffer for 10 min and then stained by sequential incubations (15 min each) with an anti-β tubulin antibody (YL1/2) and a rhodamine-conjugated, antimouse secondary antibody (*C* and *D*). The interphase extract (*A* and *C*) formed extensive membrane networks, while the metaphase extract (*B* and *D*) did not, despite the presence of similar numbers of microtubules. All panels show different, but representative fields. Bar, 5 μm.

maintained histone kinase activities that were similar to those of the extract from which they were derived (see figure legends and Materials and Methods). The crude membrane fraction, prepared by centrifugation through a 300-mM sucrose cushion, was collected from the top of the pellet, which consisted mainly of ribosomes and glycogen granules. Removing these ribosomes and glycogen particles greatly improved the visualization of microtubules and small vesicles in the reconstituted assay.

Neither the interphase nor metaphase membrane fraction was motile when incubated with microtubules in buffer plus ATP. When interphase supernatant was added to the interphase organelles, active vesicle movement and tubular membrane network formation were restored (Fig. 4 *B*, Table III). The direction of these movements was analyzed on microtubules polymerized exclusively from the plus ends of salt-extracted, sea urchin sperm axonemes (see Materials and Methods). The polarity of these microtubules was confirmed by demonstrating that carboxylated beads coated with squid kinesin (a plus end–directed motor) moved along these nucleated microtubules away from the axoneme. Vesicle movements were 68% plus end directed and 32% minus end directed (48 vesicles scored). In contrast, all tubules extended towards the microtubule minus end ($n = 45$). Minus end and plus end moving vesicles and minus end moving tubules were all transported at similar rates (1.93 ± 0.13 μm/s [± SEM, $n = 16$], 2.40 ± 0.30 μm/s [$n = 6$] and 1.75 ± 0.15 μm/s [$n = 16$], respectively).

Table II. Comparison of Tubular Membrane Network Extent in Interphase and Metaphase

Extract	Membrane tubules	Histone kinase
	μm/field	*pmol ATP/μl/min*
Interphase extract 1	203.4 ± 10.0	0.23
Interphase extract 2	133.0 ± 1.5	0.32
Metaphase extract 1	1.8 ± 1.0	10.66
Metaphase extract 2	2.3 ± 0.9	8.25

Comparison of tubular membrane network extent in interphase with that in metaphase extracts. Aliquots from two different interphase extracts prepared from activated eggs (*1* and *2*) were each treated with cyclinΔ90 (23°C for 40 min) to yield metaphase extracts (*1* and *2*). Each interphase extract and its corresponding metaphase extract was then diluted with 2 vol of acetate buffer and flowed into a perfusion chamber precoated with bovine microtubules. Membrane tubule length (25 fields per sample) was analyzed after a 10-min incubation, and the mean length per video field is expressed as μm ± SEM.

Strikingly different results were obtained using the components from metaphase extracts. Metaphase organelles combined with metaphase supernatant moved along microtubules 16-fold less frequently (0.0001 movements/μm microtubule/min: two vesicles counted over 21 min), as compared with the experiment described above in which interphase organelles were combined with interphase supernatants (0.0016 movements/μm microtubule/min: 42 vesicles counted over 24 min). In addition, membrane tubule formation was reduced by 500–1,000-fold in reactions containing metaphase supernatant and organelles compared with those containing interphase supernatants and organelles (Fig. 4 *F*; Table III).

We next investigated whether the amount of tubular membrane network formation was determined by the cell cycle state of the supernatant or the membrane fraction. When metaphase membranes were incubated with an interphase supernatant, they formed extensive tubular membrane net-

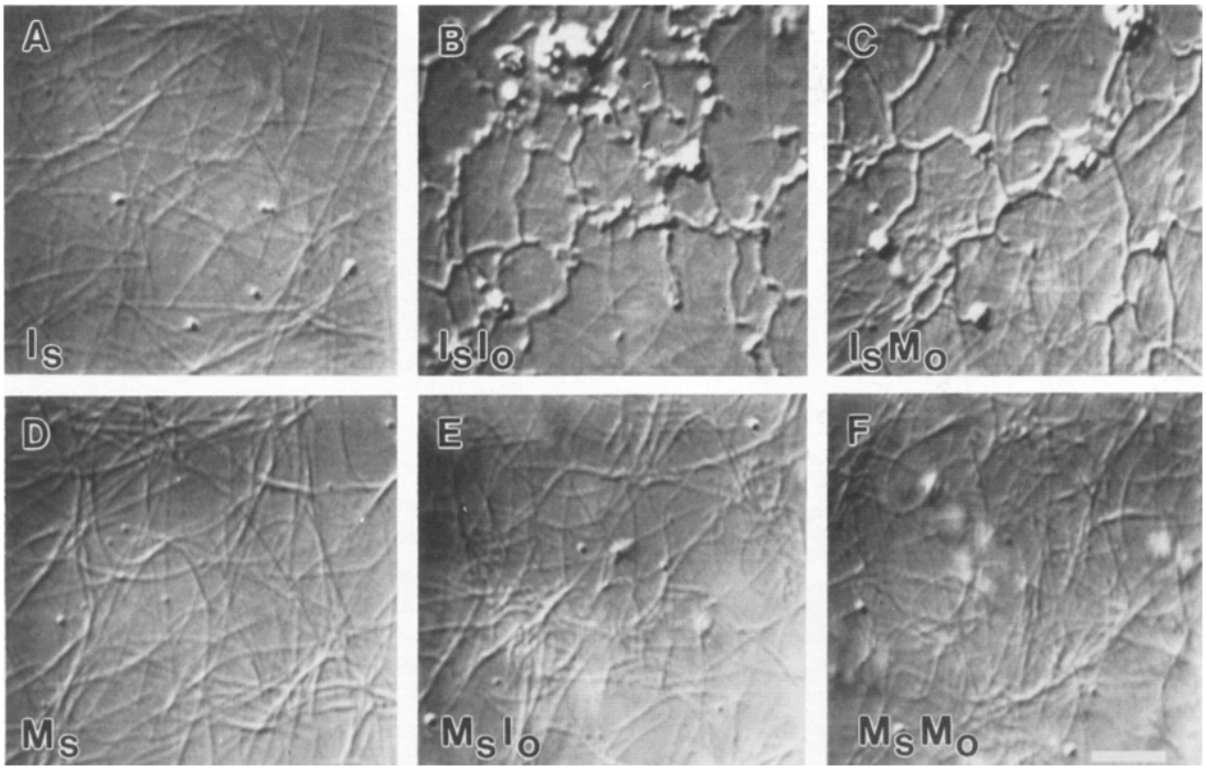

Figure 4. Xenopus soluble fractions determine the extent of membrane tubule formation from mitotic or interphase membranes. Interphase and metaphase supernatants form similar numbers of microtubules after a 30-min incubation in the perfusion chamber (*A* and *D*, respectively). Interphase supernatant promoted extensive membrane network formation when incubated for 30 min with either interphase organelles (*B*; $I_s + I_o$) or metaphase organelles (*C*; $I_s + M_o$). A metaphase supernatant, however, was unable to promote membrane network formation when incubated with metaphase (*F*; $M_s + M_o$) or interphase organelles (*E*; $M_s + I_o$). Interphase extract was prepared from activated eggs, and a portion of this extract was converted to a metaphase state by incubation with cyclinΔ90. The extracts were then used to prepare high-speed supernatant and organelle fractions, as described in Materials and Methods. High-speed supernatants (14 μl) were mixed with 2 μl of *Xenopus* organelles (or buffer) in a tube. 12 μl of the mixture was flowed into a 6-μl chamber that had been precoated with bovine microtubules; the remainder was incubated at 23°C and assayed for histone kinase activity at 30 min, the same time for which membrane tubule formation was assayed in the perfusion chamber. The histone kinase activities (pmol ATP/μl extract/min) were: *A*, 0.5; *B*, 0.3; *C*, 1.7; *D*, 7.6; *E*, 3.5; *F*, 8.1. Bar, 5 μm.

works (Fig. 4 *C*; Table III), in some cases equal to those formed with interphase organelles (Fig. 4 *B*; Table III). In contrast, the addition of interphase organelles to metaphase supernatant resulted in the formation of very few or no membrane tubules (Fig. 4 *E*; Table III). Although in both experiments the membranes affected the overall histone kinase activity, as has been observed previously (Felix et al., 1989), it was the cell cycle state of the supernatant that determined the extent of membrane tubule formation.

Since it has been postulated that the mitotic disassembly of organelles such as the Golgi apparatus occurs as a result of continued membrane budding in the absence of membrane

Table III. Formation of Membrane Tubules after Mixing Xenopus Supernatants and Membranes

Assay components	Extract 1		Extract 2	
	Tubule length	Histone kinase	Tubule length	Histone kinase
	μm/field	*pmol ATP/μl/min*	*μm/field*	*pmol ATP/μl/min*
$I_{supt} + I_{orgs}$	160 ± 13.5	0.3	187.5 ± 16.1	0.4
$I_{supt} + M_{orgs}$	162.0 ± 18.1	1.7	76.8 ± 13.2	1.2
$M_{supt} + I_{orgs}$	0.0 ± 0.0	3.5	25.9 ± 6.9	3.4
$M_{supt} + M_{orgs}$	0.3 ± 0.2	8.1	0.2 ± 0.1	3.9
M_{supt}	0	7.6	0	3.9
I_{supt}	0	0.5	0	0.5

Formation of membrane tubules after mixing *Xenopus* supernatants and membranes. Experimental procedures are described in the legend to Fig. 4. The total length of membrane tubules membrane after a 30-min incubation was analyzed for 25 fields per sample, and expressed as mean μm per field ± SEM. The data from two separate experiments are presented; the columns on the left show quantitation of the experiment depicted in Fig. 4.

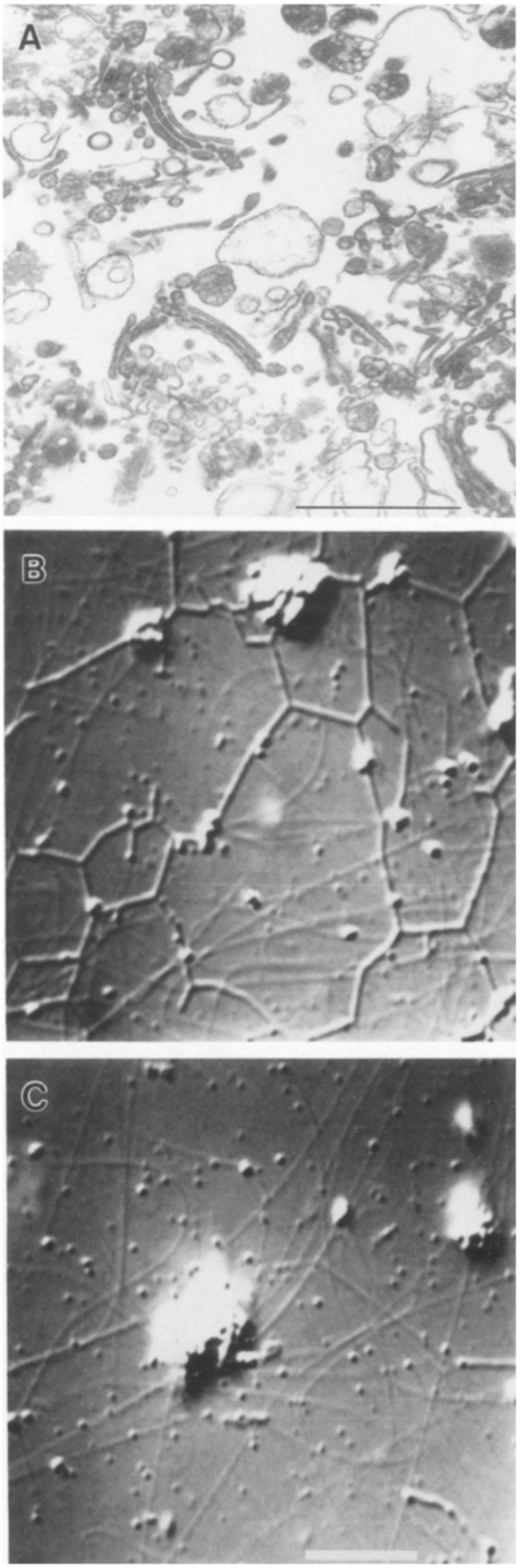

fusion (Warren, 1985), we tested whether a metaphase supernatant could fragment an interphase tubular membrane network. In this experiment, a tubular membrane network was first formed in a perfusion chamber by incubating interphase extract and microtubules for 20 min. After subsequent perfusion and incubation with a metaphase high-speed supernatant, no dissolution of the tubular network was observed (tubule length was 305.9 ± 5.9 μm/field [± SEM, n = 25] before and 282.8 ± 8.7 μm/field [n = 25] after a 20-min incubation with metaphase supernatant). Similar results were obtained when a metaphase extract was used instead of a metaphase high-speed supernatant (data not shown). Metaphase supernatants and extracts are therefore unable to disassemble preexisting interphase tubular membrane networks.

Interphase but Not Mitotic Supernatants Support Microtubule-based Transport of Rat Liver Golgi Fraction Membranes

The results described above suggest that soluble factors present in the high-speed supernatant determine whether a membrane can move along microtubules. Since changes in organelle distribution during the cell cycle occur in a wide range of higher eukaryotes, it was of interest to know whether *Xenopus* supernatant could promote motility of organelles from another species, and, if so, whether such motility is also under cell cycle control. As a source of exogenous membrane, a rat liver Golgi membrane fraction was used. This fraction contained stacked and single Golgi cisternae, secretory vesicles containing lipoprotein particles, numerous small vesicles with and without coats, and large electron-lucent membrane vesicles of unknown origin (Fig. 5 *A*).

In the presence of *Xenopus* interphase supernatant, vesicles in the rat liver Golgi fraction moved very actively along microtubules, primarily in the plus end direction (78%; n = 76 total vesicles counted). Again, the rates of minus end and plus end-directed movements were comparable (1.55 ± 0.05 μm/s [± SEM, n = 43] and 1.71 ± 0.11 μm/s [n = 18], respectively). Unlike the *Xenopus* vesicles, the Golgi fraction membranes rarely released from microtubules once they were bound, and often moved for considerable distances, switching from one microtubule to another. After a 20–30-

Figure 5. Membranes in a rat liver Golgi fraction form tubular networks in the presence of *Xenopus* interphase supernatant, but not metaphase supernatant. (*A*) An electron micrograph of the rat liver Golgi fraction reveals characteristic Golgi stacks as well as individual cisternae. Numerous coated and uncoated vesicles are found around the stacks, as are secretory vesicles containing lipoprotein particles. Larger smooth membrane vesicles and a small amount of RER are also seen. This rat liver Golgi membrane fraction formed extensive tubular networks when mixed and incubated for 60 min with a *Xenopus* interphase supernatant (*B*), but not with a mitotic supernatant (*C*). 12 μl of interphase or mitotic supernatant (prepared as described in the legend to Fig. 4) was combined with 1 μl of Golgi fraction plus 0.5 μl of sheared bovine microtubules. 10 μl was flowed into a perfusion chamber; the remainder was incubated at 23°C for 60 min in a tube and then assayed for histone kinase activity (sample containing interphase supernatant, 0.39 pmol ATP/μl extract/min; sample containing mitotic supernatant, 4.82 pmol/μl extract/min). Bars: (*A*) 1 μm; (*B* and *C*) 5 μm.

Table IV. Movement of Membranes from a Rat Liver Golgi Fraction Promoted by Xenopus Interphase or Metaphase Supernatants

Supernatant	Membrane tubule length	Histone kinase	Vesicle movements	Histone kinase
	μm/field	*pmol ATP/μl/min*	*Number/μm microtubule/min × 10³*	*pmol ATP/μl/min*
Interphase	82.0 ± 13.1	0.31 ± 0.04	18.3 ± 2.2	0.33 ± 0.03
Metaphase	9.5 ± 0.9	4.93 ± 0.76	0.3 ± 0.1	3.78 ± 0.32

Movement of membranes from a rat liver Golgi fraction promoted by either *Xenopus* interphase or metaphase supernatants. Interphase extracts were prepared from activated eggs and a portion of this extract was converted to a metaphase state with cyclinΔ90. Triplicate motility assays were performed as described in the legend to Fig. 6. The mean (± SEM) length of membrane tubules per field (30–40 fields measured per assay) was determined after 60 min. Vesicle movements per μm microtuble (MT) per min (mean ± SEM) were determined after a 10-min incubation. The values shown represent the mean (± SEM) from triplicate assays. In the three interphase assays, 27 fields were analyzed, and 358 organelles moved over 1,080 s. In three metaphase assays, the 28 fields examined revealed only five moving organelles over a 1,160-s time period. The mean (± SEM) histone kinase activities for the independent experimental determinations of membrane tubule formation and vesicle movements with interphase or metaphase supernatants are shown.

min incubation with the *Xenopus* interphase supernatant, membrane tubules began extending from aggregates of membrane attached to the glass surface (Fig. 5 *B*). These tubules moved along microtubules in the same manner as *Xenopus* membrane tubules, and also fused with one another to form polygonal networks (Fig. 5 *B*). Unlike the *Xenopus* membrane networks, the rat liver membrane tubules exhibited much less Brownian motion and appeared to be under greater tension. We were unable to determine the direction of tubule extension with respect to microtubule polarity, because microtubules nucleated from axonemes were obscured by polymerization of free, endogenous microtubules before membrane tubules began to extend. Neither tubule formation nor movement of vesicles in the Golgi fraction was seen in the absence of interphase extract, or if membranes were pretreated with trypsin. Thus, factors necessary for organelle transport in interphase *Xenopus* supernatants are able to interact with mammalian membranes and promote their movement along microtubules and their fusion to form tubular networks.

Consistent with the previous results using *Xenopus* membranes, movement of vesicles in the rat liver Golgi fraction along microtubules occurred 60-fold less frequently when they were combined with a *Xenopus* metaphase supernatant instead of an interphase supernatant (Table IV). The infrequent number of vesicle movements made it difficult to assay directionality. However, from the absolute numbers of organelles moving in the presence of interphase (358 in 1,080 s) and metaphase (5 in 1,160 s) supernatants and from the percentage of minus and plus end movements with the interphase supernatant (78% plus end), it is clear that both plus end and minus end–directed vesicle movements are reduced with metaphase supernatants. The total length of membrane tubules was also reduced ninefold (Fig. 5 *c*), and no polygonal networks were seen in the presence of the metaphase supernatant. The majority of tubules that formed in the presence of metaphase supernatant were generated by a membrane simultaneously attaching to the glass surface and to a fixed point on a microtubule and then being stretched into a tubule as the microtubule moved across the glass surface. In the presence of interphase supernatant, on the other hand, real-time observations convincingly revealed that membrane tubules form predominantly by moving actively along a microtubule.

Activity of Soluble Microtubule-based Motors

The lack of membrane tubule formation and vesicle movement in mitotic extracts or supernatants could be the consequence of an inhibition of force generation by microtubule motors. By analogy, phosphorylation has been shown to modulate the force-generating activity of smooth muscle and cytoplasmic myosins (Warwick and Spudich, 1987). To explore this possibility, the soluble microtubule motor activity in the *Xenopus* supernatants was assayed by adsorbing motor proteins either onto glass surfaces, and measuring microtubule translocation over the surface, or onto carboxylated beads, and assaying bead movement along microtubules (Vale et al., 1985*a*,*b*).

In the presence of either metaphase or interphase supernatants, microtubules nucleated from axonemes always moved on glass with their plus ends leading, indicating a relative movement of motors towards the minus end (122 and 150 microtubules observed in interphase and metaphase supernatants, respectively). Microtubule translocation on glass occurred at approximately the same rate in interphase and metaphase supernatants (Table V), and the number of moving microtubules in both cases was similar (not shown).

Carboxylated beads moved predominantly towards the microtubule minus end with interphase (92%; $n = 77$ beads) or metaphase (97%; $n = 90$ beads) supernatants. The rates of bead movement along microtubules, which were similar to the rates of membrane movement along microtubules, were comparable in interphase and metaphase supernatants (Table V). Furthermore, the number of beads moving along microtubules was similar in the presence of interphase and metaphase supernatants (0.035 and 0.021 movements/μm microtubule/min, respectively; 100 beads counted in each case).

In conclusion, despite the vast difference in the amount of microtubule-based membrane transport activity stimulated by interphase and metaphase supernatants, various parameters of soluble microtubule motor activity are comparable in these two preparations.

Discussion

Cell Cycle Regulation of Organelle Transport In Vitro

We have used *Xenopus* egg extracts to study the cell cycle

Table V. Directionality and Velocities of Vesicle, Bead, and Microtubule Movements Stimulated by Interphase or Metaphase Xenopus Supernatants

Assay	Interphase				Metaphase			
	Direction of movement		Rate of movement		Direction of movement		Rate of movement	
	plus end	minus end	plus end	minus end	plus end	minus end	plus end	minus end
	%	%	μm/s	μm/s	%	%	μm/s	μm/s
MT gliding	0	100	0	1.07 ± 0.04	0	100	0	1.21 ± 0.04
Beads	8	92	ND	2.31 ± 0.08	3	97	ND	2.37 ± 0.06
Xenopus vesicles	68	32	1.93 ± 0.13	2.40 ± 0.30	ND	ND	ND	ND
Xenopus tubules	0	100	0	1.75 ± 0.15	ND	ND	ND	ND
Golgi vesicles	78	22	1.71 ± 0.11	1.55 ± 0.05	ND	ND	ND	ND

The directionality and velocities of vesicle, bead, and microtubule movements stimulated by interphase or metaphase *Xenopus* supernatants. Supernatants were prepared as described in the Fig. 4 legend, with histone kinase activities of 0.76 and 7.75 pmol phosphate/μl extract/min for interphase and metaphase supernatants, respectively. (These values apply only to the first two rows of the table.) Total number of movements assayed for directionality: microtubule gliding, interphase and metaphase, 122 and 150, respectively; bead movements, interphase and metaphase, 77 and 90, respectively. Minus and plus indicate the direction of movement along the microtubule. Organelle motility assays are described in the text and Materials and Methods.

control of microtubule-based organelle transport and membrane tubule formation in vitro. Interphase extracts support abundant vesicle movement and membrane tubule extension along microtubules, whereas such processes are greatly reduced in metaphase extracts. These findings were substantiated using interphase and metaphase extracts prepared by different means, indicating that the level of organelle transport is truly cell cycle regulated. Extracts prepared from activated eggs that have entered interphase of their first cell cycle show considerable organelle transport activity, but after the addition of cyclin, which elevates $p34^{cdc2}$ kinase activity, membrane transport in this same extract drops precipitously. Extracts prepared from eggs arrested in the second meiotic metaphase also have high levels of $p34^{cdc2}$ kinase activity, but low levels of organelle transport along microtubules. Degradation of the endogenous cyclin in this meiotic extract after calcium addition, leads to a decrease in $p34^{cdc2}$ activity and a concomitant increase in organelle transport. The above experiments in which an extract was converted to the opposite cell cycle state were performed in the presence of cycloheximide, indicating that the control of organelle transport must occur through a posttranslational mechanism. Since many mitotic and meiotic changes are controlled by $p34^{cdc2}$ kinase (reviewed by Moreno and Nurse, 1990), it seems plausible that the mitotic inhibition of organelle transport may also be mediated by phosphorylations produced by $p34^{cdc2}$ kinase or by kinases downstream of $p34^{cdc2}$.

The cell cycle regulation of microtubule-based membrane transport appears to encompass a wide variety of organelles. The movements of two different types of *Xenopus* membranes, the membrane tubules, which move exclusively towards the microtubule minus end, and the small vesicles, which move primarily towards the plus end, are both lower in metaphase than in interphase extracts. This cell cycle regulation also extends to mammalian membranes (a rat liver Golgi fraction), which show considerable microtubule-based movement in the presence of interphase but not metaphase *Xenopus* supernatants.

The precise identities of the organelles that move in these assays have not been ascertained. The tubular membrane networks observed in the *Xenopus* extracts resemble the morphology of the ER in vivo (Terasaki et al., 1986; Lee and Chen, 1988) and of a putative ER network observed in extracts of chick fibroblasts (Dabora and Sheetz, 1988). Like the ER (Terasaki et al., 1986), the *Xenopus* membrane tubules are brightly labeled with $DiOC_6(3)$, although this lipophilic membrane dye cannot be regarded as an exclusive marker for the ER membrane. In contrast to the ER, however, which is thought to reach the cell periphery by moving along microtubules in the plus end direction (Lee et al., 1989), the *Xenopus* membrane tubules all move towards the microtubule minus end in our in vitro assay. We have also observed the formation of membrane tubules in the rat liver Golgi fraction. The *trans*-Golgi extends tubules in a microtubule-dependent manner in vivo (Cooper et al., 1990), and it is possible that we are observing this same process in vitro. However, since many other organelles have been shown recently to extend tubules in cells (Hopkins et al., 1990; Lee and Chen, 1988; Lippincott-Schwartz et al., 1990; Swanson et al., 1987), we are now using organelle-specific antibodies to establish the identity of the membrane tubules that form in these in vitro assays.

Previous studies have shown that certain membrane fusion reactions are inhibited during mitosis (Tuomikoski et al., 1989). Inhibition of membrane fusion may impair the formation of membrane-tubule networks during mitosis, but this possibility was not directly assayed in the present study. Inhibition of membrane fusion in the presence of continued vesicle budding has also been proposed as the mechanism responsible for Golgi fragmentation during mitosis (Warren, 1985). If similar processes were to occur in *Xenopus* mitotic extracts, then metaphase extracts might be expected to disassemble *Xenopus* interphase tubular membrane networks. No destabilization of previously assembled membranes was observed, however, when they were incubated with metaphase supernatants or extracts.

Cell Cycle Control of Microtubule-Membrane Interactions In Vivo

What happens to microtubule-based organelle transport during mitosis in vivo is not fully understood. Consistent with our in vitro findings, several results suggest that membrane binding to and transport along microtubules is diminished during mitosis in living cells. The interphase Golgi apparatus, for instance, moves toward the minus ends of microtubules, probably through the actions of cytoplasmic dynein (Ho et al., 1989), but the fragmented, mitotic Golgi does not appear to interact with microtubules (Lucocq et al., 1989; Robbins and Gonatas, 1964). Similarly, mitochondria, endosomes, lysosomes, and secretory granules are scattered throughout the cytoplasm during mitosis and do not appear to be microtubule associated (Lucocq et al., 1989; Matteoni and Kreis, 1987; Rebhun, 1972; Robbins and Gonatas, 1964; Tooze and Burke, 1987). Many studies have also shown that membrane traffic through the secretory and the endocytic pathways is inhibited during mitosis (Berlin and Oliver, 1978; Ceriotti and Colman, 1989; Featherstone et al., 1985; Pypaert et al., 1987; Warren et al., 1983, 1984). Such inhibition is generally attributed to an inhibition of fusion of transport vesicles between membrane compartments. However, since microtubules and motors are believed to play important roles in delivering vesicles to the cell surface (Vale, 1987) and in membrane fusion reactions (Bomsel et al., 1990), an inhibition of microtubule-based vesicle transport and tubule formation may contribute to the diminished transport through the secretory pathway during mitosis.

Several studies documenting extensive organelle transport along microtubules of the mitotic apparatus contradict the notion that membrane–microtubule interactions decrease during mitosis. The majority of these studies have come from invertebrate cells, such as the sea urchin egg (Rebhun, 1964, 1972) and *Haemanthus* (Jackson and Doyle, 1982). Electron micrographic studies have also documented associations between the ER and astral and spindle microtubules (reviewed by Hepler and Wolniak, 1984). This spindle-associated ER may play an important role in regulating calcium concentration around the mitotic apparatus.

The variation in the reports of membrane movements and locations during mitosis are difficult to reconcile. Some of the variability may reflect species differences, since the majority of studies documenting movement of membrane along astral and spindle microtubules have used invertebrate eggs. Much of the EM data is also difficult to interpret, since it does not reveal whether membrane is indeed moving on microtubules. The issues of dynamic membrane–microtubule interactions and transport during mitosis are clearly worth reexploring quantitatively in several cell types using modern methods of video-enhanced contrast microscopy. Our results predict that microtubule-based organelle transport in vertebrate cells would be reduced but not completely abolished when cells enter mitosis.

Mechanism for Cell Cycle Control of Membrane Movement and Tubule Formation

Fish melanophores regulate the direction of their microtubule-dependent granule movements through a cAMP-dependent process (Rozdzial and Haimo, 1986), but the mechanisms for controlling organelle transport in other cell types are largely unknown. A substantial decrease in cytoplasmic pH causes endosomes and lysosomes to reverse their direction of movement (Heuser, 1989), but acidification is unlikely to be a physiological means of controlling transport. This study documents one physiological cue, the interphase-mitosis transition, that regulates the movement of a variety of organelles. Both minus end and plus end–directed transport of organelles along microtubules are reduced in metaphase extracts, indicating that two different microtubule motor systems are controlled by the cell cycle.

The targets of the cell cycle–dependent, posttranslational modifications that regulate organelle transport are unknown, although several possibilities exist. The first candidates are the motor proteins themselves. Both kinesin and cytoplasmic dynein, which are likely organelle transport motors, have force-generating domains at one end of the molecule and a domain at the opposite end that may attach to organelles or a microtubule (Vale, 1991). Either domain of the molecule is a potential site of regulation. The attachment of the motor to the organelle is also thought to involve an integral membrane receptor (as yet unidentified) and perhaps other "accessory" factors that may mediate the docking reaction or may activate membrane-bound motors (Schroer et al., 1988, 1989; Schnapp and Reese, 1989). Finally, the microtubules or microtubule-associated proteins may become modified so as to inhibit the motility of motors along the microtubule substrate.

Our evidence suggests that the force-generating activities of cytoplasmic dynein, the predominant soluble motor in *Xenopus* egg extracts (see also Belmont et al., 1990), are not greatly altered during the cell cycle, at least as determined by assaying microtubule gliding on glass and bead movements along microtubules. This finding suggests that the force-generating elements of the system (the motor domain of dynein and the microtubule) are not the components being modified by the cell cycle. Owing to the paucity of kinesin-induced bead movements, our data does not address whether this motor's force-generating activity is cell cycle–controlled. It is also conceivable that the retrograde motor used for organelle transport is different from the one whose activity is measured in the soluble fraction. Despite these reservations, we feel that the interaction between motor and membrane is probably the site of cell cycle regulation. Indeed, the amount of membrane binding to microtubules is greatly reduced in metaphase extracts, suggesting that some membrane–microtubule link (possibly the motor) is inactivated. Such repression could be effected through modification of the motor's membrane-binding domain, the accessory proteins, or the membrane motor receptor. Our data does not distinguish between these possibilities.

During mitosis, motors may become dissociated from organelles and then recruited for other functions, such as constructing the mitotic spindle or moving chromosomes. The immunofluorescence localization of cytoplasmic dynein in interphase and mitosis is consistent with this overall hypothesis. During interphase, cytoplasmic dynein is found throughout the cytoplasm on punctate structures, which are thought to be membranous organelles (Pfarr et al., 1990; Steuer et al., 1990). During prophase and prometaphase, this staining is lost, and dynein localizes to kinetochores, spindle poles, and spindle microtubules (Pfarr et al., 1990;

Steuer et al., 1990). A change in the activity of cytoplasmic dynein between interphase and mitosis is also suggested by the work of Verde et al. (1991), who found that this motor promotes the aggregation of microtubules into aster structures in metaphase, but not in interphase frog egg extracts. These findings, together with the results described in this paper, suggest that the cell cycle alters the repertoire of functions served by cytoplasmic motors. The in vitro assays described here should prove useful in further dissecting the molecular mechanism that mediates the cell cycle control of microtubule motors.

We thank Michael Glotzer for providing cyclinΔ90 and the Kirschner, Murray, and Mitchison laboratories for sharing their expertise on *Xenopus* egg extracts. We are also grateful to Pete Brown for assisting with data analysis; to Debbie Crumrine for performing the EM; and to Linda Hicke for her comments on the manuscript.

This work was supported by Searle and Klingenstein Fellowships and a National Institutes of Health grant (GM38499).

Received for publication 27 November 1990 and in revised form 10 January 1991.

References

Arnheiter, H., M. Dubois-Dalcq, and R. A. Lazzarini. 1984. Direct visualization of protein transport and processing in the living cell by microinjection of specific antibodies. *Cell.* 39:99–109.

Balch, W. E. 1989. Biochemistry of interorganelle transport. A new frontier in enzymology emerges from versatile in vitro model systems. *J. Biol. Chem.* 264:16965–16968.

Belmont, L. D., A. A. Hyman, K. E. Sawin, and T. J. Mitchison. 1990. Real-time visualization of cell cycle dependent changes in microtubule dynamics in cytoplasmic extracts. *Cell.* 62:579–589.

Berlin, R. D., and J. M. Oliver. 1978. Surface functions during mitosis. I. Phagocytosis, pinocytosis and mobility of surface-bound Con-A. *Cell.* 15:327–341.

Bomsel, M., R. Parton, S. A. Kuznetsov, T. A. Schroer, and J. Gruenberg. 1990. Microtubule- and motor-dependent fusion in vitro between apical and basolateral endocytic vesicles from MDCK cells. *Cell.* 62:719–731.

Ceriotti, A., and A. Colman. 1989. Protein transport from endoplasmic reticulum to the Golgi complex can occur during meiotic metaphase in *Xenopus* oocytes: *J. Cell Biol.* 109:1439–1444.

Colman, A., E. A. Jones, and J. Heasman. 1985. Meiotic maturation in *Xenopus* oocytes: a link between the cessation of protein secretion and the polarized disappearance of Golgi apparati. *J. Cell Biol.* 101:313–318.

Cooper, M. S., A. H. Cornell-Bell, A. Chernjavsky, J. W. Dani, and S. J. Smith. 1990. Tubulovesicular processes emerge from trans-Golgi cisternae, extend along microtubules, and interlink adjacent trans-Golgi elements into a reticulum. *Cell.* 61:135–145.

Dabora, S. L., and M. P. Sheetz. 1988. Microtubule dependent formation of a tubularvesicular network with characteristics of the endoplasmic reticulum from cultured cell extracts. *Cell.* 54:27–35.

Featherstone, C., G. Griffiths, and G. Warren. 1985. Newly synthesized G protein of vesicular stomatitis virus is not transported to the Golgi complex in mitotic cells. *J. Cell Biol.* 101:2036–2046.

Felix, M.-A., J. Pines, T. Hunt, and E. Karsentì. 1989. A post-ribosomal supernatant from activated Xenopus eggs that displays post-translationally regulated oscillation of its cdc2 + mitotic kinase activity. *EMBO (Eur. Mol. Biol. Organ.) J.* 8:3059–3069.

Gibbons, I. R., and E. Fronk. 1979. A latent adenosine triphosphatase form of dynein 1 from sea urchin sperm flagella. *J. Biol. Chem.* 254:187–196.

Gruenberg, J., G. Griffiths, and K. E. Howell. 1989. Characterization of the early endosome and putative endocytic carrier vesicles in vivo and with an assay of vesicle fusion in vitro. *J. Cell Biol.* 108:1301–1316.

Hepler, P. K., and S. M. Wolniak. 1984. Membranes in the mitotic apparatus: their structure and function. *Int. Rev. Cytol.* 90:169–238.

Herman, B., and D. F. Albertini. 1984. A time-lapse video image intensification analysis of cytoplasmic organelle movements during endosome translocation. *J. Cell Biol.* 98:565–576.

Heuser, J. 1989. Changes in lysosome shape and distribution correlated with changes in cytoplasmic pH. *J. Cell Biol.* 108:855–864.

Ho, W. C., V. J. Allan, G. van Meer, E. G. Berger, and T. E. Kreis. 1989. Reclustering of scattered Golgi elements occurs along microtubules. *Eur. J. Cell Biol.* 48:250–263.

Hollenbeck, P. J., and J. A. Swanson. 1990. Radial extension of macrophage tubular lysosomes supported by kinesin. *Nature (Lond.).* 346:864–866.

Hopkins, C. R., A. Gibson, M. Shipman, and K. Miller. 1990. Movement of internalized ligand-receptor complexes along a continuous endosomal reticulum. *Nature (Lond.).* 346:335–339.

Huttner, W. B., W. Schiebler, P. Greengard, and P. De Camilli. 1983. Synapsin 1 (protein 1), a nerve terminal-specific phosphoprotein. III. Its association with synaptic vesicles studied in a highly purified synaptic vesicle population. *J. Cell Biol.* 96:1374–1388.

Jackson, W. T., and B. G. Doyle. 1982. Membrane distribution in dividing endosperm cells of *Haemanthus. J. Cell Biol.* 94:637–643.

Lee, C., M. Ferguson, and L. B. Chen. 1989. Construction of the endoplasmic reticulum. *J. Cell Biol.* 109:2045–2055.

Lee, C. H., and L. B. Chen. 1988. Behavior of endoplasmic reticulum in living cells. *Cell.* 54:37–46.

Leelavathi, D. E., L. W. Estes, D. S. Feingold, and B. Lombardi 1970. Isolation of a Golgi-rich fraction from rat liver. *Biochim. Biophys. Acta.* 211:124–138.

Lippincott-Schwartz, J., J. G. Donaldson, A. Schweizer, E. G. Berger, H.-P. Hauri, L. C. Yuan, and R. D. Klausner. 1990. Microtubule-dependent retrograde transport of proteins into the ER in the presence of Brefeldin A suggests an ER recycling pathway. *Cell.* 60:821–836.

Lohka, M. J., and J. L. Maller. 1985. Induction of nuclear envelope breakdown, chromosome condensation, and spindle formation in cell-free extract. *J. Cell Biol.* 101:518–523.

Lucocq, J. M., E. G. Berger, and G. Warren. 1989. Mitotic Golgi fragments in HeLa cells and their role in the reassembly pathway. *J. Cell Biol.* 109:463–474.

Matteoni, R., and T. E. Kreis. 1987. Translocation and clustering of endosomes and lysosomes depends on microtubules. *J. Cell Biol.* 105:1253–1265.

Moreno, S., and P. Nurse. 1990. Substrates for $p34^{cdc2}$: in vivo veritas? *Cell.* 61:549–551.

Murray, A., and M. Kirschner. 1989. Cyclin synthesis drives the early embryonic cell cycle. *Nature (Lond.).* 339:275–280.

Murray, A., M. Solomon, and M. W. Kirschner. 1989. The role of cyclin synthesis in the control of maturation promoting factor activity. *Nature (Lond.).* 246:614–621.

Newport, J. 1987. Nuclear reconstitution in vitro: stages of assembly around protein-free DNA. *Cell.* 48:205–217.

Newport, J., and T. Spann. 1987. Disassembly of the nucleus in mitotic extracts: membrane vesicularization, lamin disassembly, and chromosome condensation are independent processes. *Cell.* 48:219–230.

Nurse, P. 1990. Universal control mechanism regulating onset of M-phase. *Nature (Lond.).* 344:503–508.

Paschal, B. M., H. S. Shpetner, and R. B. Vallee. 1987. MAP1C is a microtubule-activated ATPase which translocates microtubules in vitro and has dynein-like properties. *J. Cell Biol.* 105:273–1282.

Pfarr, C. M., M. Coue, P. M. Grissom, T. S. Hays, M. E. Porter, and J. R. McIntosh. 1990. Cytoplasmic dynein is localized to kinetochores during mitosis. *Nature (Lond.).* 345:263–265.

Pfister, K. K., M. C. Wagner, D. L. Stenoien, S. T. Brady, and G. S. Bloom. 1989. Monoclonal antibodies to kinesin heavy and light chains stain vesicle-like structures, but not microtubules, in cultured cells. *J. Cell Biol.* 108: 1453–1463.

Pypaert, M., J. M. Lucocq, and G. Warren. 1987. Coated pits in interphase and mitotic A431 cells. *Eur. J. Cell Biol.* 45:23–29.

Rambourg, A., and Y. Clermont. 1990. Three-dimensional electron microscopy: structure of the Golgi apparatus. *Eur. J. Cell Biol.* 51:189–200.

Rebhun, L. I. 1964. Saltatory particle movements and their relation to the mitotic apparatus. *In* Primitive Motile Systems in Cell Biology. R. D. Allen and N. Kamiya, editors. Academic Press, New York. 503–525.

Rebhun, L. I. 1972. Polarized intracellular particle transport: saltatory movements and cytoplasmic streaming. *Int. Rev. Cytol.* 32:3–137.

Robbins, E., and N. K. Gonatas. 1964. The ultrastructure of a mammalian cell during the mitotic cycle. *J. Cell Biol.* 21:429–463.

Roos, U.-P. 1973. Light and electron microscopy of rat kangaroo cells in mitosis. I. Formation and breakdown of the mitotic apparatus. *Chromosoma (Berl.).* 40:43–82.

Rozdzial, M. M., and L. T. Haimo. 1986. Bidirectional pigment granule movements of melanophores are regulated by protein phosphorylation and dephosphorylation. *Cell.* 47:1061–1070.

Sagata, N., N. Watanabe, G. F. Vande Woude, and Y. Ikawa. 1989. The c-mos proto-oncogene product is a cytostatic factor (CSF) responsible for meiotic arrest in vertebrate eggs. *Nature (Lond.).* 342:512–518.

Schnapp, B. J., and T. S. Reese. 1989. Dynein is the motor for retrograde axonal transport of organelles. *Proc. Natl. Acad. Sci. USA.* 86:1548–1552.

Schroer, T. A., B. J. Schnapp, T. S. Reese, and M. P. Sheetz. 1988. The role of kinesin and other soluble factors in organelle movement along microtubules. *J. Cell Biol.* 107:1785–1792.

Schroer, T. A., E. R. Steuer, and M. P. Sheetz. 1989. Cytoplasmic dynein is a minus-end-directed motor for membranous organelles. *Cell.* 56:937–946.

Sheetz, M. P., S. M. Block, and J. A. Spudich. 1986. Myosin movement in vitro: a quantitative assay using oriented actin cables from *Nitella. Methods Enzymol.* 134:531–544.

Steuer, E. R., L. Wordeman, T. A. Schroer, and M. P. Sheetz. 1990. Localization of cytoplasmic dynein to mitotic spindles and kinetochores. *Nature (Lond.).* 345:266–268.

Swanson, J., E. Burke, and S. C. Silverstein. 1987. Tubular lysosomes accom-

pany stimulated pinocytosis in macrophages. *J. Cell Biol.* 104:1217–1222.
Terasaki, M., L. B. Chen, and K. Fujiwara. 1986. Microtubules and the endoplasmic reticulum are highly interdependent structures. *J. Cell Biol.* 103: 1557–1568.
Tooze, J., and B. Burke. 1987. Accumulation of adrenocorticotropin secretory granules in the midbody of telophase AtT20 cells: evidence that secretory granules move anterogradely along microtubules. *J. Cell Biol.* 104:1047–1057.
Tuomikoski, T., M.-A. Felix, M. Doree, and J. Gruenberg. 1989. Inhibition of endocytic vesicle fusion in vitro by the cell-cycle control protein kinase cdc2. *Nature (Lond.).* 342:942–945.
Vale, R. D. 1987. Intracellular transport using microtubule-based motors. *Annu. Rev. Cell Biol.* 3:347–378.
Vale, R. D. 1991. Severing of stable microtubules by a mitotically-activated protein in Xenopus egg extracts. *Cell.* 64:827–840.
Vale, R. D., and H. Hontani. 1988. Formation of membrane networks in vitro by kinesin-driven microtubule movement. *J. Cell Biol.* 107:2233–2242.
Vale, R. D., and Y. Y. Toyoshima. 1988. Rotation and translocation of microtubules in vitro induced by dyneins from *Tetrahymena* cilia. *Cell.* 52: 459–469.
Vale, R. D., T. S. Reese, and M. P. Sheetz. 1985*a*. Identification of a novel force-generating protein, kinesin, involved in microtubule-based motility. *Cell.* 42:39–50.
Vale, R. D., B. J. Schnapp, T. Mitchison, E. Steuer, T. S. Reese, and M. P. Sheetz. 1985*b*. Different axoplasmic proteins generate movement in opposite directions along microtubules in vitro. *Cell.* 43:623–632.
Verde, F., J. Labbe, M. Doree, and E. Karsenti. 1990. Regulation of microtubule dynamics by cdc2 protein kinase in cell-free extracts of Xenopus eggs. *Nature (Lond.).* 343:233–238.
Verde, F., J.-M. Berrez, C. Antony, and E. Karsenti. Taxol-induced microtubule asters in mitotic extracts of *Xenopus* eggs: requirement for phosphorylated factors and cytoplasmic dynein. 112:1177–1187.
Warren, G. 1985. Membrane traffic and organelle division. *TIBS (Trends Biochem. Sci.).* 10:439–443.
Warren, G., C. Featherstone, G. Griffiths, and B. Burke. 1983. Newly synthesized G protein of vesicular stomatitis virus is not transported to the cell surface during mitosis. *J. Cell Biol.* 97:1623–1628.
Warren, G., J. Davoust, and A. Cockcroft. 1984. Recycling of transferrin receptors in A431 cells is inhibited during mitosis. *EMBO (Eur. Mol. Biol. Organ.) J.* 3:2217–2225.
Warwick, H. M., and J. A. Spudich. 1987. Myosin structure and function in cell motility. *Annu. Rev. Cell Biol.* 3:379–422.
Zeligs, J. D., and S. H. Wollman. 1979. Mitosis in rat thyroid epithelial cells in vivo. I. Ultrastructural changes in cytoplasmic organelles during the mitotic cycle. *J. Ultrastruct. Res.* 66:53–77.